Proceedings of the 28th IEEE
EMBS Annual International Conference
New York City, USA, Aug 30-Sept 3, 2006

Fabrication of Polymer Neural Probes with Sub-cellular Features for Reduced Tissue Encapsulation

John P. Seymour, *Student Member, IEEE,* and Daryl R. Kipke, *Member, IEEE*

Abstract— **Intracortical microelectrodes currently have great potential as a neural prosthesis in patients with neurodegenerative disease or spinal cord injury. In an effort to improve the consistency of neural probe performance, many modifications to probe design are focused on reducing the tissue encapsulation. Since researchers have shown that small polymer fibers (less than 7-µm diameter) induce a small to non-existent encapsulation layer in the rat subcutis [1, 2], we have proposed a neural probe design with similarly small diameter structures. This paper discusses the fabrication and design parameters of a microscale neural probe with a sub-cellular lattice structure.**

We developed a microfabrication process using SU-8 and parylene-C to create the relatively thick probe shank and thin lateral arms. The stiff penetrating shank (70-µm by 42-µm) had an SU-8 core that allowed control over stiffness and simplified the process. Parylene-only structures lateral to the shank could be defined with a 4-µm feature-size to meet our sub-cellular criterion. We fabricated four varying geometries for implantation into the neocortex of seven Sprague-Dawley rats. Our *in vivo* testing verifies that despite the flexible substrate and small dimensions (4-µm x 5-µm), these devices are mechanically robust and practical as neural probes. These devices provide an important tool for neural engineers to investigate the tissue response around sub-cellular structures and potentially improve device efficacy.

I. Introduction

The failure mode of chronic neural probe recordings has been linked to the foreign body response. Histological examination has consistently shown that a glial scar forms around the probe tract [3-5]. An increase in electrical impedance is concomitant with the time course of this reactivity and is therefore believed to be the cause of attenuated and noisy signal recordings [6-8]. Researchers are investigating a variety of techniques to prevent neuronal loss and cellular encapsulation by modulating the acute immune response and long-term reactivity [9].

This experiment investigates the feasibility of a novel probe geometry in an effort to improve microelectrode longevity. Our probe design was inspired by other biomaterial studies on the adhesion and reactivity to a material's shape and size. Researchers have reported a marked decrease in cellular encapsulation when small diameter polymer fibers (less than 7-µm) were implanted in the rat subcutis [1, 2]. Similarly, cells do not adhere well to small adhesive pads or small glass beads (less than 10-µm) *in vitro* [10]. In these and other studies, geometry was the critical parameter in determining the cellular response and revealed that sub-cellular geometry can modulate mechanotransduction [11].

A structure that is both sufficiently stiff for cortical penetration and sufficiently fine to meet the sub-cellular criterion has not yet been developed. We propose a conventional backbone or shank geometry, but with an adjoining lattice structure (see Figure 1). We believe this design provides a new tool to investigate the tissue response in the central nervous system and may provide improved chronic recordings.

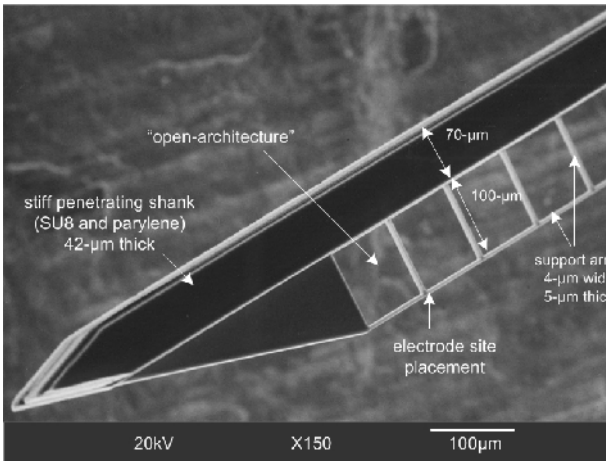

Fig. 1. SEM of an open-architecture parylene neural probe (tip is shown). The primary design principle is to move the electrical/chemical sensing site to the lateral edge of a fine lattice structure where cellular encapsulation is expected to be less dense. A critical parameter is the support arm dimensions and in this case is 4-µm by 5-µm.

II. Methods

A. Device Fabrication

A graphical description of the fabrication process is shown in Figure 2. (1) A sacrificial release layer of SiO_2 is grown on a 4-inch Si wafer. Parylene-C (5-µm) is deposited

Manuscript received April 24, 2006. This work was supported in part by the National Institutes of Health, Grant 401415-1 and by the Engineering Research Centers program of the National Science Foundation under NSF Award Number EEC-9986866.

J. P. Seymour is with the Biomedical Engineering Department, University of Michigan, Ann Arbor, MI 48109 USA (e-mail: seymourj@umich.edu).

D. R. Kipke is also with the Biomedical Engineering Department, University of Michigan, Ann Arbor, MI 48109 USA (e-mail: dkipke@umich.edu).

via chemical vapor deposition (PDS-2010, Indianapolis, IN). (2) A Ti layer (1000Å) is deposited and patterned for later use as mask for the sub-cellular lattice structure. (3) AP-300 (Silicon Resources, Chandler, AZ), a titanium oxide solution, is spun on as a base adhesion layer. SU-8 2025 (Microchem, Newton, MA) is spun on at 32-µm and patterned to create the core of the probe shank. Oxygen plasma RIE surface treatment occurs before and after the SU-8 layer to improve interfacial adhesion. (5) The second parylene layer is deposited 5-µm thick. This film conforms to the SU-8 backbone. To pattern the shank of the probe, we spun multiple layers of AZ-9260 resist (Clariant) to cover the SU-8 structure (~70-µm thick). (6) Parylene was etched using oxygen plasma RIE. Devices were released using hydrofluoric acid and then rinsed in DI water, ethanol, and acetone. Since this experiment was not intended to record biopotentials, this process did not include electrodes. Electrode metallization in future runs will occur between steps (1) and (2) above for optimal lithography.

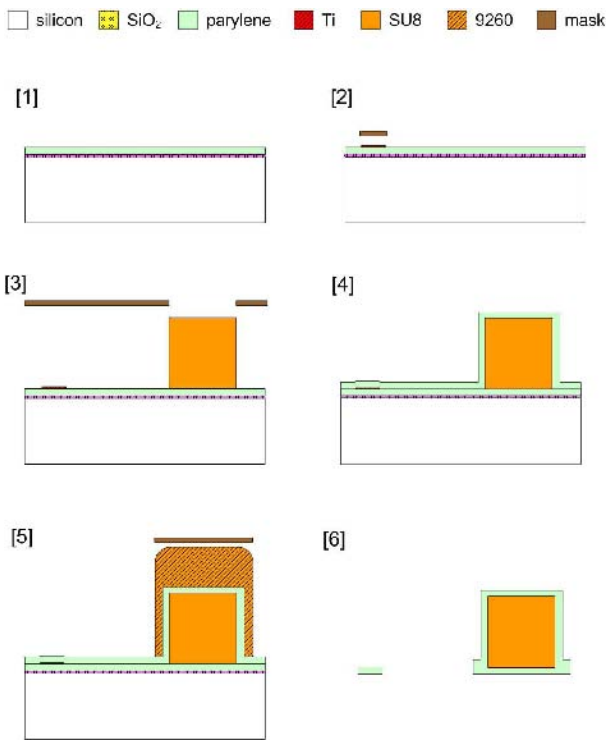

Fig. 2. Microfabrication of open-architecture polymer neural probe (approx. to scale). This process enables designers to create large variations in structure thickness on the same device with high precision lithography. We have created 4-µm by 5-µm features attached to a rigid shank. See text for fabrication details.

B. Assembly

Each probe was mounted on a custom Ni-alloy plate (shown in Fig. 3) using poly-ethyl glycol (PEG, 8000 M.W.) as a water-soluble glue. The plates were machined with a notch to secure the head of the probe. This assembly was then sterilized and mounted on a stereotaxic frame to allow precise positioning and a controlled trajectory during insertion.

C. Surgical Procedure

Nine male Sprague Dawley rats (300-400 grams) were implanted with four parylene probes. Anesthesia was administered using intra-peritoneal injections of a mixture of ketamine, xylazine, and acepromazine. A craniotomy was created over the motor cortex and the dura resected. The pia was left intact and undamaged in all cases. After the electrodes were inserted via the stereotaxic frame, ALGEL® was applied, followed by silicone and dental acrylic (Co-Oral-Ite Dental Mfg. Co.) [12]. These probes were nonfunctional so that the implant was almost entirely intraparenchymal and thereby reduce the confounding effects of transcranial tethering. Less than 400-µm of the device was above the brain surface.

The mechanical integrity of these structures was verified *in situ* during the histological investigation in nine of the animals. The probe structure was also monitored during insertion with a 3X microscope.

III. Results

A. Mechanical Stability as a Neural Probe

More than forty parylene devices, all 2.1-mm long, have been implanted in live anesthetized animals with no mechanical failure. We tested devices with varying feature size in several acute and nine chronic preparations. The smallest dimensions tested were 3-µm x 5-µm with a lattice structure described in Fig. 1 and inserted at least once in each animal. Despite the flexibility of the 5-µm thick parylene structures extending 100-µm from the stiff penetrating shank, none of these features bent or buckled.

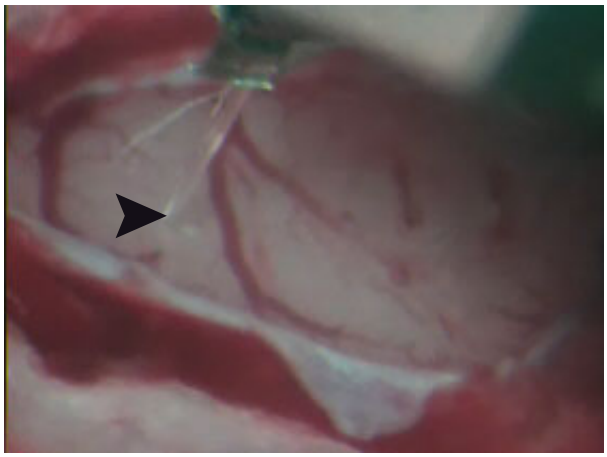

Fig. 3. Sample image taken during insertion of parylene neural probe into rat neocortex. Tip of device (black arrow) is chisel-shaped to reduce dimpling when piercing the pia mater. Although the sub-cellular features are relatively flexible, the insertion forces are focused at the tip. Ni-alloy assembly plate (top of image) is secured to a stereotaxic frame. Image taken at 3X.

These surgeries prove a 4-µm x 5-µm lateral structure made

of parylene (Young's modulus = 3GPa) is sufficiently stiff for intracortical probes when coupled with a 42-µm x 70-µm x 2.1-mm shank. All of the probes tested had the same tip shape (13 degrees, chisel-shaped). Dimpling rarely occurred during insertion (probably due to the presence of blood vessels near the pial surface); and when dimpling did occur, the mild depression did not produce bleeding. Acute preparations tested the insertion, retraction and re-insertion of the devices with no change in dimpling or damage after multiple trials.

Table 1 compares some common neural probe materials and geometries to the shank dimension used in this design, which forms the leading edge and backbone to this polymer structure. As shown, the designed stiffness is comparable to silicon "Michigan" probes.

Table 1
Comparison of neural probe stiffness assuming rectangular cantilever

Sample Neural Probes	E (GPa)	t (µm)	w (µm)	k (mN/m)
Tungsten microwire	406	20	20	601
Silicon single shank "Michigan" array [a]	133	15	140	62
SU-8 shank [b]	2.5	42	70	72

Length assumed to 3mm for each
[a] Assumed to be boron-doped silicon throughout
[b] Parylene-C has a slightly higher Young's modulus of 3.2GPa

B. Histology

Cryosections reveal these structures remain intact. Figure 4 shows the transverse cross-section through a probe four weeks after implantation. This transverse pattern was seen on each probe with a 4-µm x 5-µm lateral structures evaluated at four weeks and was consistent along the entire length of the shank. This indicates that any bending or curling that may have occurred was manageable. Another advantage of a polymer-based probe is that when cryosectioned, the device/tissue interface is left intact.

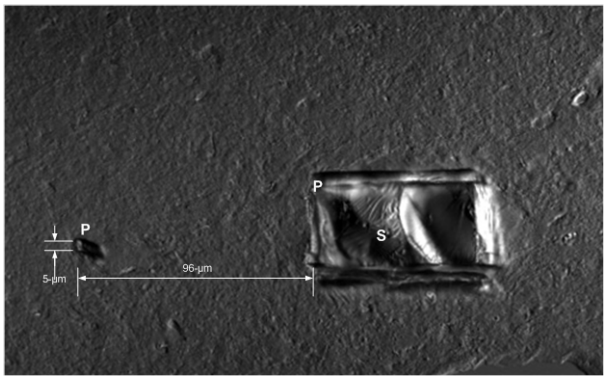

Fig. 4. Differential interference contrast image (400X) of a transverse cross-section of the probe and 4-µm x 5-µm lattice structure. The measurements shown were made with calibrated microscopy software. The lateral edge was expected to be 100 microns from the edge of the shank. This indicates that any bending or curling that may have occurred was small. Tissue/device contrast images support the video evidence taken during surgery that no mechanical damage occurred.

Early immunohistochemical results reveal less encapsulation at the lateral edge of these devices. Notice in Figure 5 that there is a high density of cell nuclei surrounding the shank of the device and very few surrounding the lateral edge. Also seen in this image, the neuronal loss around the shank extends further from the shank relative to the sub-cellular structure, where there are nearby viable neurons. This fluorescent image is representative of the response seen in two of the seven animals. The other five animals all had less encapsulation around the shank, but none exhibited encapsulation around the lateral edge. These early results support the hypothesis of reduced encapsulation at the lateral edge and around sub-cellular features.

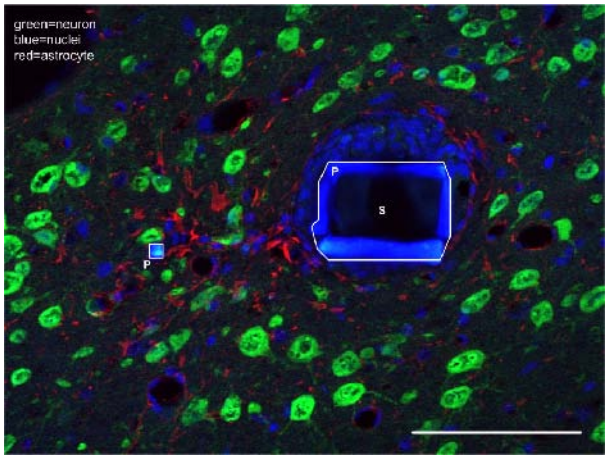

Fig. 5. Transverse fluorescent confocal image (400X, oil immersion). NeuN+ (green, neuronal nuclei), GFAP+ (red, astrocytes) and Hoechst counter stain (blue) around the neural probe. The shank is shown on right (white box) and consists of parylene (P) encasing SU-8 (S). The 4x5-µm lateral edge on left is parylene only. Notice the difference in encapsulation density and thickness surrounding the two structures. Neurons are also seen adjacent to the fine lateral structure, but none around the shank. Scale bar = 100µm.

IV. Conclusion

These results suggest that using MEMS-based microfabrication to create sub-cellular structures for implantation in the rodent model is feasible. We also believe this concept of sub-cellular features and lateral electrode placement could be beneficial to any implantable sensor capable of scaled geometries.

V. Future Work

The histological results from these implants are currently under analysis. A quantitative analysis of the neuronal and non-neuronal densities is expected to provide more details about the response. A variety of other devices created using this process is currently being evaluated, including a passive drug delivery probe and a neural stem cell delivery probe.

Acknowledgment

We would like to thank David Pellinen and staff at the Michigan Nanofabrication Facility for clean room training and fabrication advice.

References

1. Sanders, J.E., et al., *Small fiber diameter fibro-porous meshes: Tissue response sensitivity to fiber spacing.* J Biomed Mater Res A, 2005. **72A**(3): p. 335-42.
2. Sanders, J.E., C.E. Stiles, and C.L. Hayes, *Tissue response to single-polymer fibers of varying diameters: evaluation of fibrous encapsulation and macrophage density.* J Biomed Mater Res, 2000. **52**(1): p. 231-7.
3. Stensaas, S.S. and L.J. Stensaas, *The reaction of the cerebral cortex to chronically implanted plastic needles.* Acta Neuropathol (Berl), 1976. **35**(3): p. 187-203.
4. Biran, R., D.C. Martin, and P.A. Tresco, *Neuronal cell loss accompanies the brain tissue response to chronically implanted silicon microelectrode arrays.* Exp Neurol, 2005. **195**(1): p. 115-26.
5. Szarowski, D.H., et al., *Brain responses to micro-machined silicon devices.* Brain Res, 2003. **983**(1-2): p. 23-35.
6. Liu, X., et al., *Stability of the interface between neural tissue and chronically implanted intracortical microelectrodes.* IEEE Transactions on Rehabilitation Engineering, 1999. **7**(3): p. 315-26.
7. Ludwig, K.A., et al., *Chronic neural recordings using silicon microelectrode arrays electrochemically deposited with a poly(3,4-ethylenedioxythiophene) (PEDOT) film.* J Neural Eng, 2006. **3**(1): p. 59-70.
8. Rousche, P.J. and R.A. Normann, *Chronic recording capability of the Utah Intracortical Electrode Array in cat sensory cortex.* Journal of Neuroscience Methods, 1998. **82**(1): p. 1-15.
9. Polikov, V.S., P.A. Tresco, and W.M. Reichert, *Response of brain tissue to chronically implanted neural electrodes.* J Neurosci Methods, 2005. **148**(1): p. 1-18.
10. Chen, C.S., et al., *Geometric control of cell life and death.* Science, 1997. **276**(5317): p. 1425-8.
11. Chen, C.S., J. Tan, and J. Tien, *Mechanotransduction at cell-matrix and cell-cell contacts.* Annu Rev Biomed Eng, 2004. **6**: p. 275-302.
12. Vetter, R.J., et al., *Chronic neural recording using silicon-substrate microelectrode arrays implanted in cerebral cortex.* IEEE Trans Biomed Eng, 2004. **51**(6): p. 896-904.